

# Impacts of the North Atlantic subtropical high on interannual variation of summertime heat stress over the conterminous United States

Wenhong Li<sup>1</sup> · Tian Zou<sup>1,2</sup> · Laifang Li<sup>1</sup> · Yi Deng<sup>3</sup> · Victor T. Sun<sup>4</sup> · Qinghong Zhang<sup>2</sup> · J. Bradley Layton<sup>5</sup> · Soko Setoguchi<sup>6</sup>

Received: 27 June 2018 / Accepted: 1 March 2019 © Springer-Verlag GmbH Germany, part of Springer Nature 2019

#### **Abstract**

Heat index (HI) provides a proven indicator of heat stress and discomfort for the general public. The index takes the integrated effects of both temperature and humidity into account, and both factors are regulated by large-scale circulation patterns. This study examines the *impacts of the North Atlantic Subtropical High (NASH) on HI over the* conterminous *United States (CONUS)*. *The* analysis suggests that the HI is primarily controlled by surface air temperature over the CONUS; but is negatively correlated with relative humidity in the western and Central US north of 40°N. In addition, winds contribute to the variation of HI in the Midwest and the southeastern US. By regulating these meteorological parameters, the movement of the NASH western ridge significantly impacts HI over the US, especially the Southeast. When the NASH western ridge is located northwest (NW) of its climatological mean position, abnormally high temperatures are observed due to fewer clouds and a precipitation deficit, leading to positive HI anomalies over the southeastern US. In contrast, when the western ridge is located in the southwest (SW), temperature decreases and HI anomaly becomes negative over the Southeast, even though relative humidity increases east of 100°W. NASH has a weaker impact on the HI when it is far from the North American continent, especially during southeast (SE) ridge years. In the future, CMIP5 models project an increase in HI over the entire CONUS, while NASH-induced HI will be weakened during the NW, SE and NE ridge years but strengthened when its ridge moves to the SW quadrant. These results suggest that future increases in heat stress are likely caused by climatological warming and NASH intensification.

**Keywords** US heat waves · Heat index · North Atlantic subtropical high · NASH western ridges

**Electronic supplementary material** The online version of this article (https://doi.org/10.1007/s00382-019-04708-1) contains supplementary material, which is available to authorized users.

Wenhong Li wenhong.li@duke.edu

Published online: 08 March 2019

- Earth and Ocean Sciences, Nicholas School of the Environment, Duke University, Durham, NC, USA
- Department of Atmospheric and Oceanic Sciences, School of Physics, Peking University, Beijing, China
- School of Earth and Atmospheric Sciences, Georgia Institute of Technology, Atlanta, GA, USA
- <sup>4</sup> John Dewey Academy, Great Barrington, MA, USA
- <sup>5</sup> RTI Health Solutions, Research Triangle Park, NC, USA
- Institute for Health, Health Care Policy and Aging Research, Rutgers Biomedical and Health Sciences, New Brunswick, NJ, USA

#### 1 Introduction

Throughout history, the United States (US) has experienced detrimental heat waves (Knowlton et al. 2009; Westcott 2011; Peterson et al. 2013; Smith et al. 2013; Berko et al. 2014; Vanos et al. 2015; National Weather Service 2017), which harm sensitive populations especially the elderly and people with pre-existing health conditions (Gao et al. 2012). For example, the 1995 Chicago heat wave claimed hundreds of lives (Whitman et al. 1997); in 2014, more than 400 Minnesotans went to the emergency department, and two died from hear-related illness (Minnesota Department of Health 2015). As the climate warms in the future, more intense heat waves are likely to occur (Meehl and Tebaldi 2004; Ganguly et al. 2009), causing extensive human suffering and economic loss.

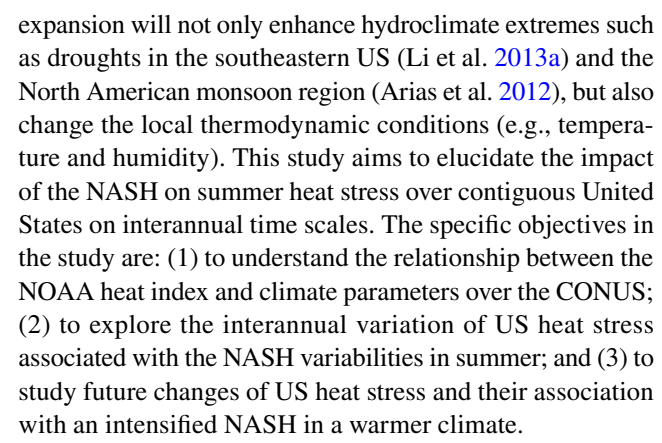


Extreme heat waves generally occur in summer and are usually associated with large-scale displacement of air masses (Grotjahn et al. 2016). In summer, as the jet stream weakens and moves poleward, the weather and climate in the US are strongly influenced by the North Atlantic Subtropical High (NASH) (Davis et al. 1997; Li et al. 2011; Arias et al. 2012). The NASH, also known as the Bermuda High, is a semi-permanent high-pressure system over the North Atlantic Ocean in the lower troposphere (Nigam and Chan 2009). In boreal summer, the high-pressure system intensifies, and its western ridge extends into the eastern coast of the US. The variabilities of the NASH intensity and location significantly impact summertime weather and climate in the US, especially the regional hydroclimate over the Southeastern US, Central US and North American monsoon region (Stahle and Cleaveland 1992; Davis et al. 1997; Gamble and Curtis 2008; Li et al. 2011; Arias et al. 2012; Wei et al. 2018a, b). Previous studies found that when the NASH western ridge is located to the southwest of its climatological mean position, excessive precipitation is observed in the eastern US due to increased moisture transported from adjacent tropical oceans. In contrast, when the western ridge is located in the northwest, a precipitation deficit prevails over the southeastern US because of the subsidence, clear skies, and prolonged dry conditions at the surface produced by the high-pressure system (Li et al. 2012a).

The impact of NASH on precipitation is mainly associated with the unique circulation dynamics along its western ridge, i.e., the balance between the stretch of the vortex tube and the advection of planetary vorticity. Such rich features of circulation dynamics along the NASH western ridge can influence atmospheric temperature directly through temperature advection and adiabatic heating/cooling and indirectly through the radiative processes associated with convection and precipitation (Trenberth and Shea 2005). The impact of the NASH on heat stress and associated physical mechanisms over the contiguous United States (CONUS), however, has not yet been systematically investigated.

Generally, atmospheric high-pressure systems have strong influence on atmospheric humidity, temperature, and winds (Wallace and Hobbs 2006). When an area is controlled by a high-pressure system, it is difficult for other weather systems, especially cyclones, to move into the region. As a result, heat waves can last for several days, or even weeks. Further, the high-pressure system inhibits winds, making them faint to nonexistent. In addition, high-pressure systems also prevent the formation of clouds, allowing increased direct sunlight which heats the region even more. The combination of these effects often induces exceptionally hot weather.

In the future as the climate warms, the NASH is projected to be intensified, and its western ridge is predicted to move further westward by state-of-the-art global climate models (Li et al. 2012b). The intensified NASH and its westward



The manuscript is organized as follows: in Sect. 2, data and methods employed in the study are introduced. In Sect. 3, results about the relationship between the heat index and climate variables as well as heat stress associated with the NASH are presented. Concluding remarks are included in Sect. 4.

### 2 Data and methods

The heat index (HI) analyzed in this study, also known as the apparent temperature, was developed by George Winterling and was adopted by the USA's National Weather Service in 1979. HI is an index to illustrate the human body's comfort, and it is what the temperature feels like to the human body when relative humidity is combined with the air temperature (Steadman 1979). Such a definition has important considerations for the human body's comfort, and HI is calculated as follows:

$$\begin{split} \text{HI} &= -42.379 + 2.04901523 \text{T}_{\text{as}} + 10.14333127 \text{RH} \\ &- 0.22475541 \text{T}_{\text{as}} \text{RH} - 6.83783 \times 10^{-3} \text{T}_{\text{as}}^{2} \\ &- 5.481717 \times 10^{-2} \text{RH}^{2} + 1.22874 \times 10^{-3} \text{T}_{\text{as}}^{2} \text{RH} \\ &+ 8.5282 \times 10^{-4} \text{T}_{\text{as}} \text{RH}^{2} - 1.99 \times 10^{-6} \text{T}_{\text{as}}^{2} \text{RH}^{2} \end{split}$$

where T<sub>as</sub> is air temperature in Fahrenheit, and RH is relative humidity expressed as a percentage (%). In this study, we use the daily maximum temperature following Russo et al. (2017). Our results and overall conclusion are quite similar when using daily mean air temperature (not shown). Daily maximum temperature is obtained from 1218 stations in The United States Historical Climatology Network (US-HCN, Quinlan et al. 1987; Easterling et al. 1996); relative humidity (RH) is derived from the National Center for Environmental Prediction/National Center for Atmospheric Research (NCEP/NCAR) Reanalysis dataset (Kalnay et al. 1996) during the 1950–2017 period. Compared to observed RH from 171 weather stations over the continuous US at the World Meteorological Organization (WMO) webpage https://web.



archive.org/web/20160630125021/http://data.un.org/Data.aspx?d=CLINO&f=ElementCode%3a11, NCEP/NCAR reanalysis generally capture the pattern of RH—the spatial correlation between the two is 0.87; however, the reanalyzed RH is overestimated by about 4–5% over the southeast, northeast and Midwest compared to observation (Supplementary). As the aim of the paper is to understand the interannual changes in summertime HI induced by the NASH in the current and future climate, we focused on the summer (June–July–August) mean HI instead of daily extremes during the 1950–2017 period.

Following previous studies (Li et al. 2012a, 2013a; Wei et al. 2018a), the NASH and associated atmospheric circulation and cloud amount are analyzed using NCEP/NCAR reanalysis (Kalnay et al. 1996) and by the International Satellite Cloud Climatology Project (ISCCP) Stage D2 data from 1984 to 2009 (Rossow and Schiffer 1991), respectively. We utilized NCEP/NCAR reanalysis data due to its relatively longer temporal coverage, and the consistency between NCEP/NCAR and the other more up-to-date reanalysis datasets in quantifying the NASH variability has been confirmed (Li et al. 2011, 2013b).

The ISCCP cloud amount data are de-trended to avoid spurious long-term changes caused by satellite artifacts (Clement et al. 2009). The summer mean (June–July–August) records during 1984–2009 are analyzed in this study due to the data availability. Cloud amount derived from the Moderate Resolution Imaging Spectroradiometer (MODIS) data and the *Clouds* and the Earth's Radiant Energy System (CERES) during 2000–2017 are also analyzed to compare the cloud coverage variation associated with different NASH ridge types.

The 850-hPa geopotential height has been chosen in this study to avoid complications due to possible topographic effects on the western edge of the NASH. The ridge-line of the subtropical highs is where winds with an easterly component reverse to winds with a westerly component (Fig. 1), and thus mathematically fulfills u = 0 and  $\frac{\partial u}{\partial y} > 0$ , where u is the zonal wind component (Liu and Wu 2004). Following Li et al. (2011), the western ridge is defined as the point of intersection between the 1560-gpm isopleth and the above-defined ridge line (Fig. 1).

In order to analyze the relationship between the NASH variation and summer HI over the conterminous US, we categorize the ridge locations according to their relative position to the climatological mean NASH western ridge (86°W, 27°N) during 1950–2017, and divide its area of influence into four different quadrants: northeast (NE), northwest (NW), southwest (SW), and southeast (SE) types, respectively. Composite analysis of the heat index and climate variables related with the HI such as air temperature (T<sub>as</sub>), wind, and relative humidity (RH) are

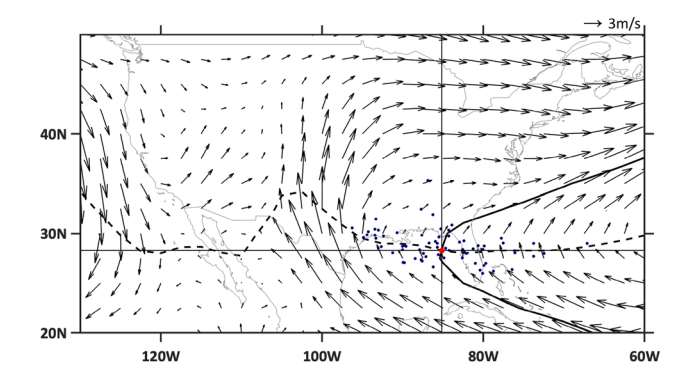


**Fig. 1** Spatial distributions of the NASH western ridge position (blue dots), together with the climatological mean position (86°W, 27°N, red dot), the 850-hPa wind field (vectors), the 1560-gpm isoline of 850-hPa geopotential height (bold curve) and the 850-hPa subtropical high ridge line (dashed curve) during the period 1950–2017

analyzed based on the ridge types. Among the 68 summers, the numbers of NW, SW, NE and SE type of NASH western ridge are 21, 16, 10 and 21, respectively.

In the future, as the climate warms, the NASH is projected to be strengthened (Li et al. 2012a, b). The HI changes associated with an intensified NASH are analyzed using CMIP5 model output under the historical (1950–1999) and the Representative Concentration Pathways 8.5 (RCP8.5) scenario (2050–2099). The historical experiments represent the current climate which are driven by observed changes in atmospheric composition (Taylor et al. 2012). In the RCP 8.5, greenhouse gas emissions continue to rise throughout the twenty-first century and the radiative forcing values will be increased by 8.5 W/m² in the year 2100 relative to pre-industrial values (Taylor et al. 2012).

In this study, the multi-model ensemble (MME) is applied to project future climate. The MME emphasizes HI changes due to climate forcing and deemphasizes differences in models' dynamic cores and parameterization schemes (Gleckler et al. 2008). Of the 29 CMIP5 models, 16 are chosen because these models reasonably capture the climatology and interannual variations of HI, T<sub>as</sub>, and RH compared to observations (Table 1), and the pattern correlations between the simulation and observation are higher than their lower quartile, i.e., 0.76, 0.69, and 0.73 for HI, T<sub>as</sub> and RH, respectively over CONUS. The overall results are similar when using a stricter standard to choose models; although there is some improvement of the HI climatology and the relationship between HI and NASH in the Historical scenario, fewer "good" models make it hard to pass the significant test. We employ one member of each model (r1i1p1) in the study following Biasutti and Giannini (2006).



Table 1 CMIP5 models in study

Model	Modeling center	Correlation coefficient w/ observation		
		HI	T <sub>as</sub>	RH
ACCESS1-0	CSIRO-BOM	0.81	0.79	0.84
ACCESS1-3		0.82	0.70	0.90
CCSM4	NCAR	0.85	0.76	0.87
CESM1-BGC	NSF/DOE NCAR	0.84	0.74	0.85
CESM1-CAM5		0.84	0.79	0.84
CNRM-CM5	CNRM-CERFACS	0.77	0.75	0.74
CSIRO-Mk3-6-0	CSIRO-QCCCE	0.77	0.70	0.81
GFDL-CM3	NOAA GFDL	0.87	0.77	0.74
GFDL-ESM2G		0.85	0.79	0.83
GFDL-ESM2M		0.87	0.76	0.74
GISS-E2-H	NASA GISS	0.85	0.79	0.87
GISS-E2-R		0.86	0.74	0.82
GISS-E2-R-CC		0.86	0.74	0.81
HadGEM2-AO	MOHC	0.83	0.76	0.76
MIROC5	MIROC	0.81	0.73	0.90
NorESM1-M	NCC	0.80	0.79	0.87

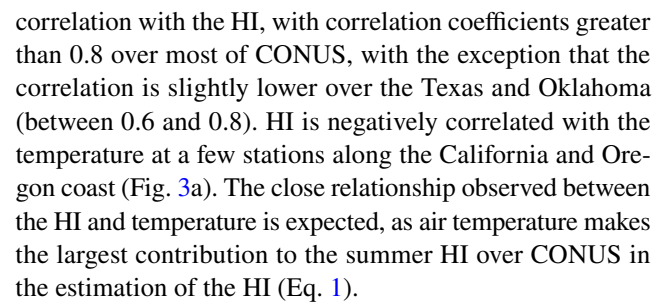
Correlation coefficients of HI, T<sub>as</sub> and RH between each model and observation are also listed (see details in Sect. 2)

#### 3 Results

# 3.1 Relationship between the heat index and climate parameters over the CONUS

Figure 2a shows the climatology of the HI during June–July–August (JJA) over the CONUS. In boreal summer, the HI value tends to decrease with latitude (Fig. 2a). Specifically, HI is highest in the southeastern and southwestern US, with HI maximized in Florida, Georgia, South Carolina, Alabama, Mississippi, Louisiana, Southern Texas, and the stations at the boundary of Arizona and Southern California. Lower HIs are observed in the northern US including the Central US, Pacific Northwest, New York, Minnesota and Wisconsin, where the HI value is usually lower than 82 °F. In addition, the standard deviation of the summer HI suggests that the interannual variability of HI is higher east of the 100°W, especially over the southeastern US where standard deviation of the HI is greater than 7.2 °F (Fig. 2b). Comparatively, there is less HI variability over the Western US. Overall, Fig. 2 suggests that the Southeastern US experiences the highest HI and the strongest variability during 1950-2017.

In order to further understand the relationships between the HI and meteorological variables, the correlations between the HI and temperature, relative humidity, and low-troposphere winds over the CONUS are calculated and shown in Fig. 3. Overall, temperature has the highest



Compared to temperature, relative humidity is less well-correlated with HI and shows mostly a negative correlation in the Northern US (Fig. 3b). The negative correlation is most significant over the Western and Central US north of  $40^{\circ}$ N, where the correlation coefficient is between -0.4 and -0.8 (Fig. 3b). The correlation coefficient between RH and the HI becomes weakly positive in the Southwestern US (Fig. 3b).

Besides the two thermodynamic variables, winds also indirectly contribute to the variation of the HI over the Great Plains, Midwest, and Eastern US. The correlation between the HI and 850-hPa wind speed is positive over the US. Midwest and northern Central US (Fig. 3c). The positive correlation is more significant in the states of Nebraska, South Dakota, Iowa, and southern Minnesota, indicating that stronger southerly winds (Fig. 1) are linked to higher HI values and is presumably due to the advection of warm, moist air by the southerly wind (Fig. 3c) associated with the NASH in the region (Wei et al. 2018b). In contrast, HI shows a negative correlation with the wind speed at the stations in the eastern US especially in Georgia, Alabama, Mississippi, Indiana, Ohio, West Virginia, Pennsylvania and New York (Fig. 3c).

In summary, the HI is primarily controlled by surface air temperature in the CONUS; relative humidity shows a negative correlation with the HI in the Western and Central US north of 40°N. Figure 3 also illustrates that atmospheric winds play a role over the Midwest and eastern US, suggesting that the interannual variation of the HI involves dynamic processes.

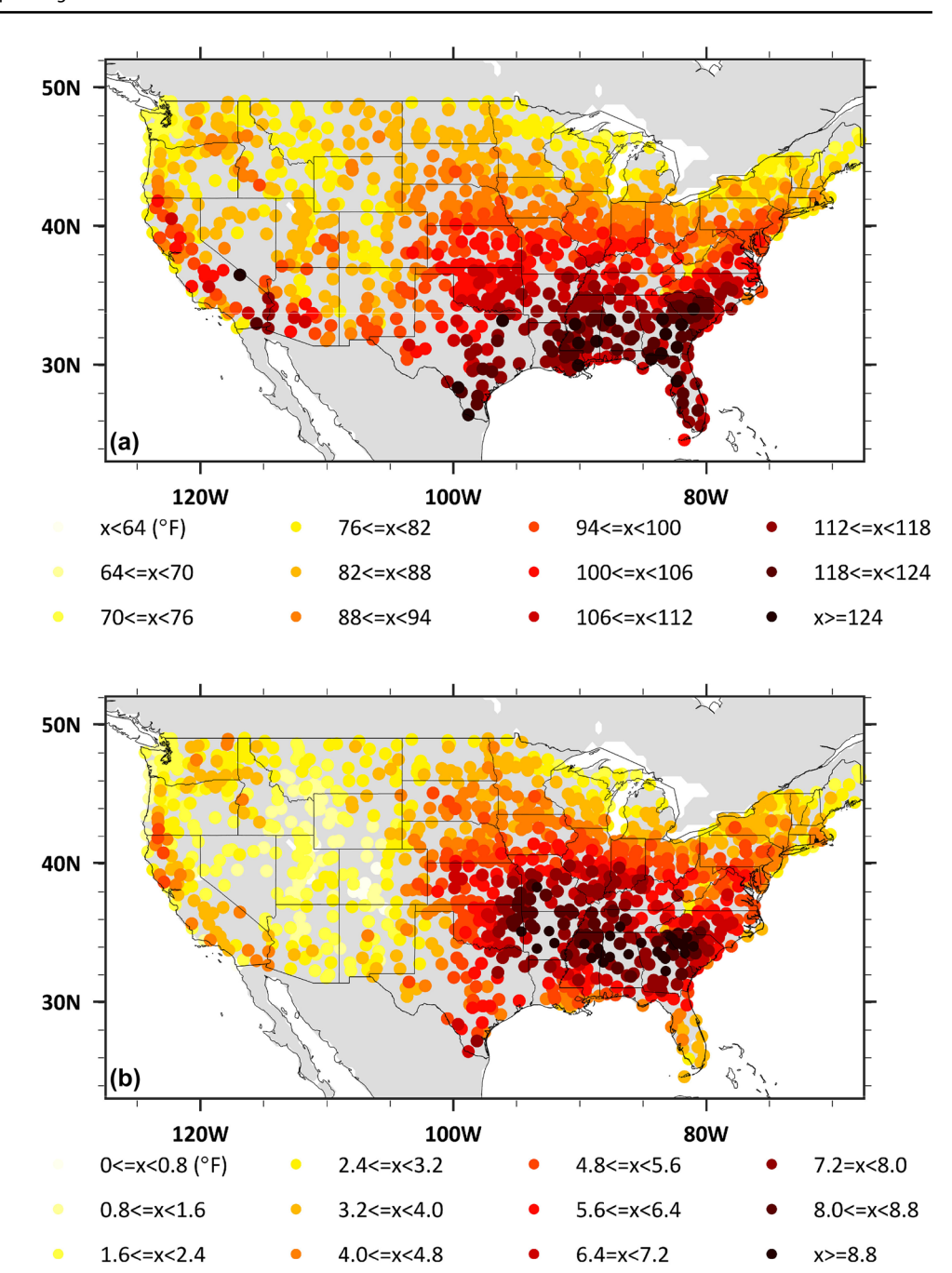
### 3.2 Variations of the NASH western ridge and its impact on the US heat index

Results from Sect. 3.1 demonstrate that interannual variations of the HI are not only affected by the variation in thermodynamic variables ( $T_{as}$  and RH), but also that dynamic parameters (winds) indirectly influence the HI. This naturally suggests a strong link between the HI and the NASH whose variation generates climate impacts both thermodynamically and dynamically (Li et al. 2015).

There has been considerable interannual variation of the NASH intensity and associated atmospheric circulation in recent decades (Li et al. 2011). When the NASH intensifies,



**Fig. 2** Summertime (June–July–August) HI over the US during 1950–2017 **a** climatology, and **b** standard deviation (unit: °F)



its western boundary expands more westward to the North American continent; whereas the western boundary associated with a weaker NASH tends to retreat eastward (Li et al. 2011, 2012b). Thus, the movement of the NASH will likely alter the abovementioned thermodynamic and dynamic variables that affects HI (Arias et al. 2012; Wei et al. 2018b).

## 3.2.1 Interannual variations of HI associated with the NASH variability

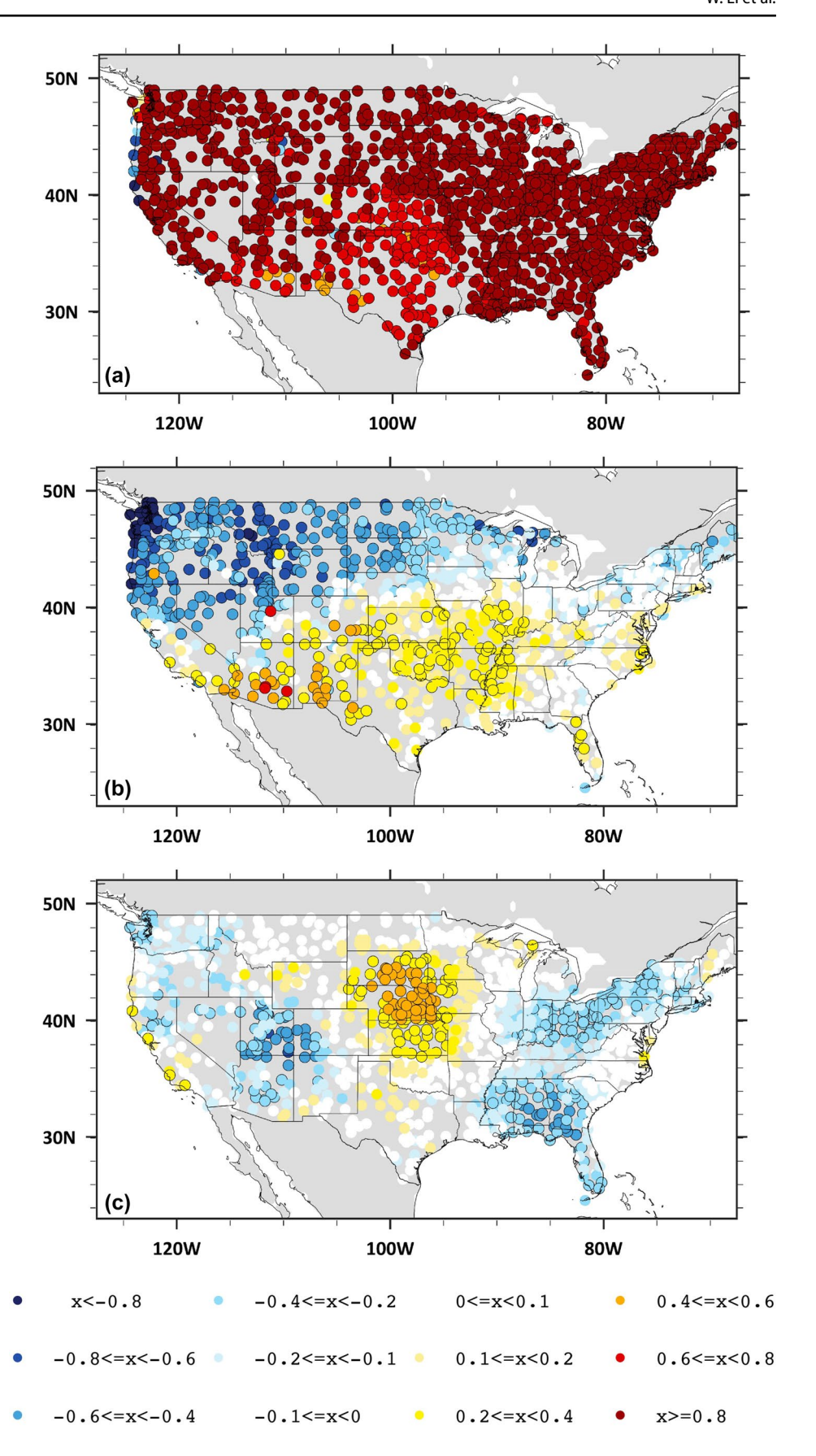
Figure 4 shows the composite of US summer HI on the four NASH western ridge locations. The northwest ridge pattern

corresponds to positive HI anomalies over the southeastern US, where the HI anomalies exceed 2 °F except Florida (Fig. 4a). Over Missouri and Arkansas, positive HI anomalies are also observed. The spatial distribution of HI anomalies (Fig. 4a) shares some similarities to the negative precipitation anomalies (Li et al. 2012b) and positive temperature anomalies (Fig. 5a) over the region, which increases the heat stress during the NW ridge position years (Fig. 4a).

HI anomalies corresponding to the southwest (SW) ridge type exhibit the opposite pattern of those corresponding to the NW ridge type (Fig. 4b). Negative HI anomalies are mainly located east of 100°W, whereas



Fig. 3 Correlation coefficient between the HI and **a** T<sub>as</sub>, **b** RH, and **c** total wind speed at 850-hPa. Stations passing 95% confidence level are plotted with black circles





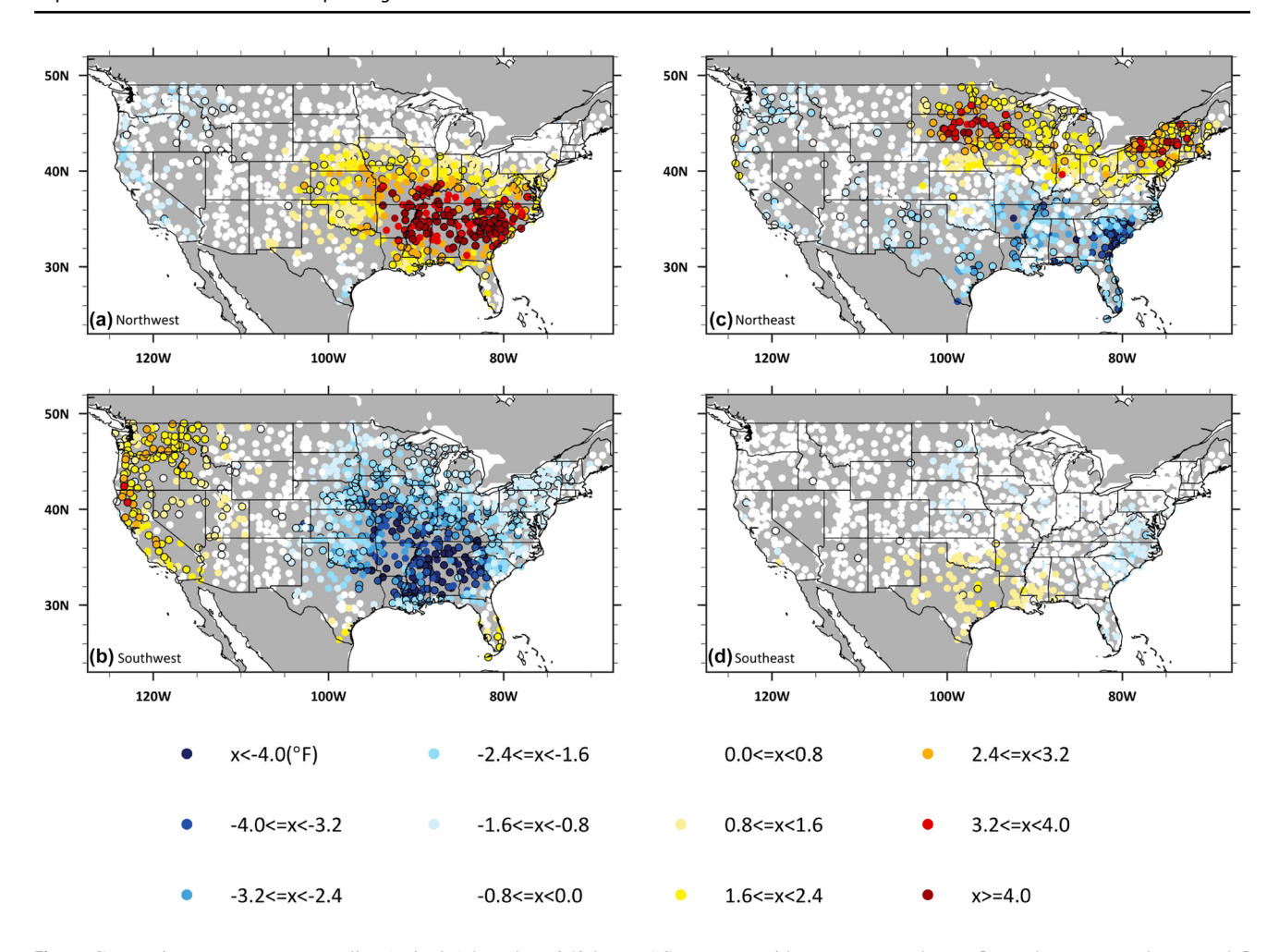


Fig. 4 Composite summer HI anomalies (unit: °F) based on 850-hPa NASH western ridge types **a** northwest, **b** southwest, **c** northeast, and **d** southeast, respectively. Stations passing 95% confidence level are plotted with black circles

positive anomalies are observed only over the Pacific northwest and California. The HI anomalies are below -3 °F in most of the southeastern US states. Figure 4a, b demonstrates a strong response of the HI to the meridional migration of the NASH western ridge when the ridge extends westward.

When the western ridge retreats eastward, its impacts on CONUS HI are weaker (Fig. 4c, d). Specifically, when the ridge is located in the northeast (NE) quadrant relative to its climatological mean position, HI is characterized by weak negative anomalies over the Southeastern US, and positive anomalies over the Northern US east of 105°W (Fig. 4c). HI anomalies become negative in Georgia and South Carolina. The HI anomalies are weakest when the NASH western ridge is located in the southeast (SE) quadrant (Fig. 4d), indicating that NASH has little impact on the HI when far from the North American continent with its ridge southward.

# 3.2.2 Through what parameters/processes does the NASH ridge control the heat index over the US?

To elucidate the mechanism through which NASH impacts the HI, we analyze the changes of T<sub>as</sub>, RH, and winds associated with NASH western ridge position. We focus on the NW- and SW-ridge not only because these two ridge types have greater impact on CONUS HI than their eastward counterparts, but also because their occurrence is likely to increase in the future as climate warms (Li et al. 2013b).

Figure 5 shows the  $T_{as}$  variations associated with the four different ridge types. When the NASH ridge is located in the NW quadrant, positive  $T_{as}$  anomalies can be observed over the Southeastern US, and negative anomalies can be observed over the Northwestern US. Over the Southeastern US and central Great Plains,  $T_{as}$  is about 0.6–1 °F above summer climatology. The spatial pattern of the  $T_{as}$  anomalies resembles that of the HI (Fig. 4a), suggesting the importance



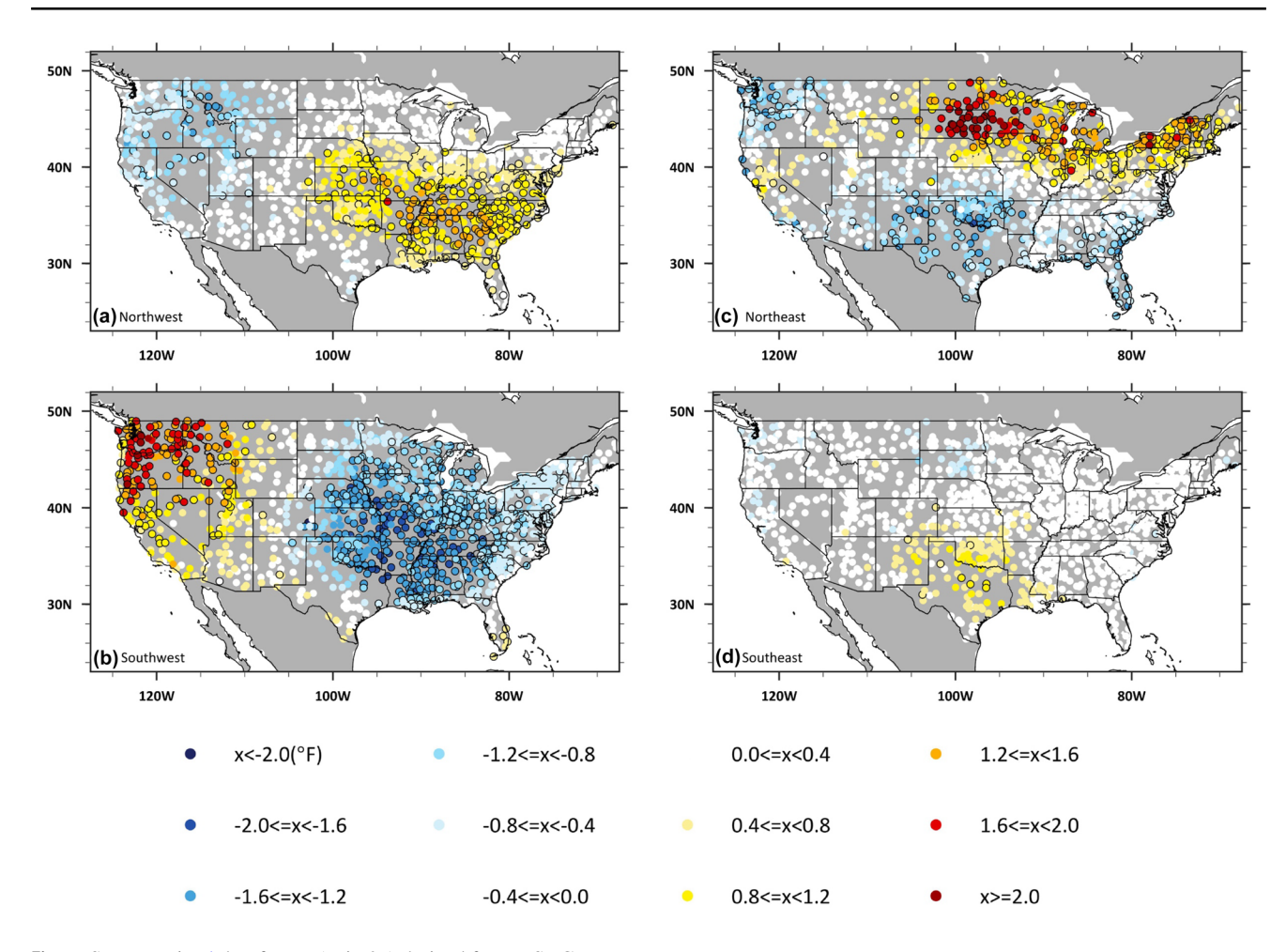


Fig. 5 Same as Fig. 4, but for  $T_{as}$  (unit: °F) derived from USHCN

of temperature variation in heat index changes. In the northwestern US,  $T_{as}$  is below normal by 0.4–0.6 °F which is insignificant (Fig. 4a).

 $T_{as}$  responses to the SW, NE, and SE ridges (Fig. 5b–d) are also similar to the HI anomalies (Fig. 4b–d). When the NASH ridge is located in the SW quadrant,  $T_{as}$  anomalies tend to be negative over the US east of 100°W, but they are positive over the Pacific Northwest (Fig. 5c). When the NASH ridge is in the NE quadrant, temperature is above normal by 0.6–1 °F over the north Central, north Midwest and Northeastern US, and  $T_{as}$  anomalies are negative over southern US and Pacific Northwest (Fig. 5b).  $T_{as}$  anomalies are almost zero over the entire CONUS when the NASH ridge is in its SE quadrant (Fig. 5d). Figures 4 and 5 suggest that the position of the NASH western ridge is closely linked to the observed variability in HI by altering atmospheric temperature ( $T_{as}$ ), since  $T_{as}$  is a primary factor to determine the strength of HI (Eq. 1).

The temperature impact on HI, however, can be modified by the RH whose changes are subject to the spatial variation of the NASH western ridge (Fig. 6). Generally, RH anomalies are stronger when the NASH western ridge is located in the NW, SW, and NE quadrants (Fig. 6a-c) compared to the ridge in the SE quadrant (Fig. 6d). Different from the T<sub>as</sub> responses to the NW ridge type which is more apparent over southeastern US (Fig. 5a), positive RH anomalies are mainly observed over northwestern US, especially over Idaho; NW ridge location has a minor impact on the RH over the Central and Eastern US (Fig. 6a). When the ridge places at the SW and NE directions relative to its climatological position, the responding RH patterns are similar to those of T<sub>as</sub> (Fig. 5b, c), but in the opposite direction (Fig. 6b, c). RH positive anomalies is much stronger in the CONUS east of 100°W during the SW-ridge years. The opposite sign of RH and T<sub>as</sub> anomalies corresponding to these NASH ridge types reflects an inverse relationship between local relative humidity and temperature (Aguado and Burt 2015). Figure 6 suggests that the heat stress modulated by local RH is likely through variations of T<sub>as</sub> during SW- and NE-ridge years.

Wind also varies with the movement of the NASH western ridge (Li et al. 2011), as shown in Fig. 7. The summer atmospheric circulation with the NW-type ridge is



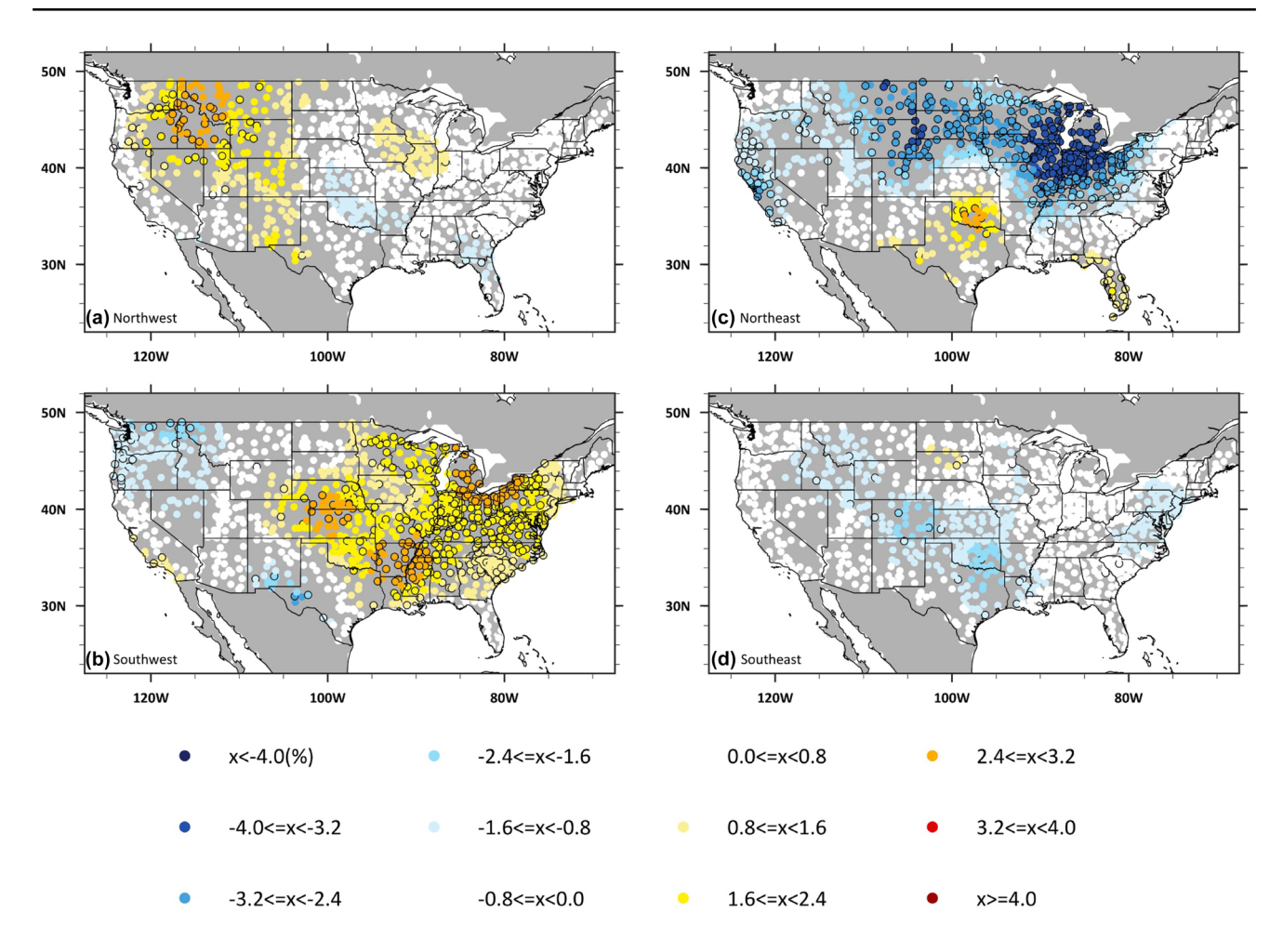


Fig. 6 Same as Fig. 4, but for surface relative humidity (unit: %) derived from NCEP/NCAR reanalysis

characterized by an intensification of the Great Plains low level jet (GPLLJ) and an abnormal anticyclonic circulation over the Central and Southeastern US (Fig. 7a). Such abnormally strong southerly winds carry tropical warm air to the Great Plains and Midwest (Ting and Wang 1997; Wei et al. 2018b), which increases temperatures (Fig. 5a) but has less of an impact on humidity (Fig. 6a). Thus, the meridional wind is positively correlated with the HI (Fig. 3c), contributing to an increased heat stress over the region (Fig. 7a). The anticyclonic circulation over the southeastern US also inhibits local vertical motion, prevents clouds formation, and allows sunlight to further heat up the land surface. Indeed, the cloud coverage decreases over the southeastern US in the NW-ridge years (Fig. 8a). All these processes lead to increased T<sub>as</sub> and HI over the central and southeastern US (Figs. 4a, 5a).

In contrast, when the NASH western ridge moves to the SW quadrant, an anomalous cyclonic circulation can be found over the Great Plains and Southeastern US (Fig. 7b). With the same mechanism in action, a decreased HI will be observed. This result agrees with the analysis by Li et al.

(2012a) which found that the SW ridging corresponds to wetter than normal summers, resulting in relatively higher clouds (Fig. 8b), colder  $T_{as}$  and negative HI anomalies over the regions (Figs. 4b, 5b).

When the NASH western ridge is located in the NE quadrant, different wind anomaly patterns are found over the Northern and Southern US east of 100°W (Fig. 7c). Specifically, in the Northern US (40°N northward) and east of 100°W, abnormally anticyclonic flows can be observed. Such wind patterns lead to higher T<sub>as</sub> (Fig. 5c) over Midwest due to decreased cloud amount (Fig. 8c), deficit rainfall (Li et al. 2012a), and increased surface insolation (not shown). The abnormally high T<sub>as</sub> contributes to a higher HI over the region (Fig. 4c). Similarly, abnormally cyclonic flows correspond to negative T<sub>as</sub> and weaker heat stress (Fig. 4c) over the southern US east of 100°W. During the SE ridge years when the high-pressure system is far from the North American continent, atmospheric winds do not vary much compared to the climatology (Fig. 7d), and the impact of the NASH circulation on HI is minimal. These results are supported by the CERES/MODIS cloud data during 2000–2017,



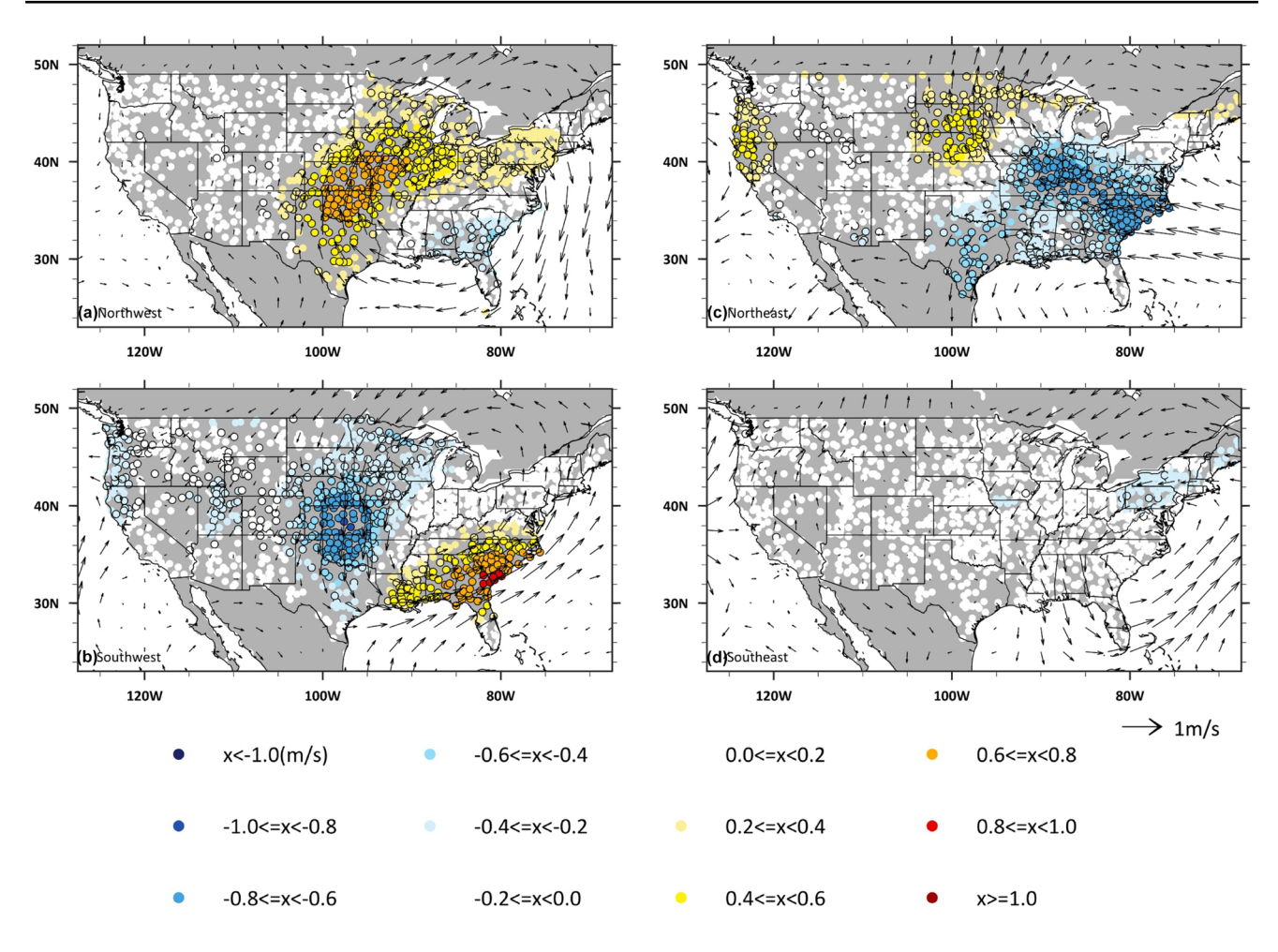


Fig. 7 Same as Fig. 4, but for 850-hPa wind speed (unit: m/s, colored) and wind field (vectors)

especially when the western ridge is located in the NW and SW quadrants (not shown).

#### 3.3 Future changes of heat index over the CONUS

In the future as the climate warms, atmospheric temperature will increase over the entire CONUS according to the CMIP5 models (Wuebbles et al. 2013; Intergovernmental Panel on Climate Change 2014), potentially increasing the HI. Figure 9 shows changes in summer HI from 1950 to 1999 to 2050–2099. The multimodel ensemble (MME) mean HI increases over the entire CONUS, especially east of 105°W; and future HI will be 21% higher over southeastern US.

The background warming alters the NASH circulation (Li et al. 2011, 2012b, 2013b) and can potentially change the way NASH influences the interannual variation of the HI over CONUS. Figure 10 shows the CMIP5 model-simulated HI anomalies based on different NASH ridge types during 1950–1999. In comparison with the historical observations (Fig. 4), the modeled HI show similar patterns corresponding to the four ridge types especially when the NASH ridge

sits in the NW (Fig. 10a) or SW quadrant (Fig. 10b). NW and SW ridge types correspond to higher and lower HI anomalies, respectively, over the area east of the 100°W; and the pattern correlation (0.7 for NW and 0.69 for SW) between the modeled and observed HI is statistically significant at the 0.05 level, taking into account the spatial correlation between meteorological variables (Dave et al. 2012). Simulated HI is underestimated, especially over the Midwest and Northeast US, when the NASH is located in the NE quadrant (Fig. 10c); contrarily, modeled HI is significant overestimated for the SE-type ridge (Fig. 10d). On average, the magnitude of modelled HI anomalies is about 51%, 90% and 240% weaker in the NW, SW, SE ridge years, but it is about three and a half times stronger in the SE ridge years.

In the future as greenhouse gas concentration increases, NASH will be intensified and move further westward (Li et al. 2012b), leading to an increased number of NW and SW ridge years (Fig. 11). Specifically, the NW-type and SW-type ridges are projected to increase by 67% and 80%, respectively, under the RCP8.5 scenario compared to Historical scenario, where the SE- and NE-type ridges decrease by



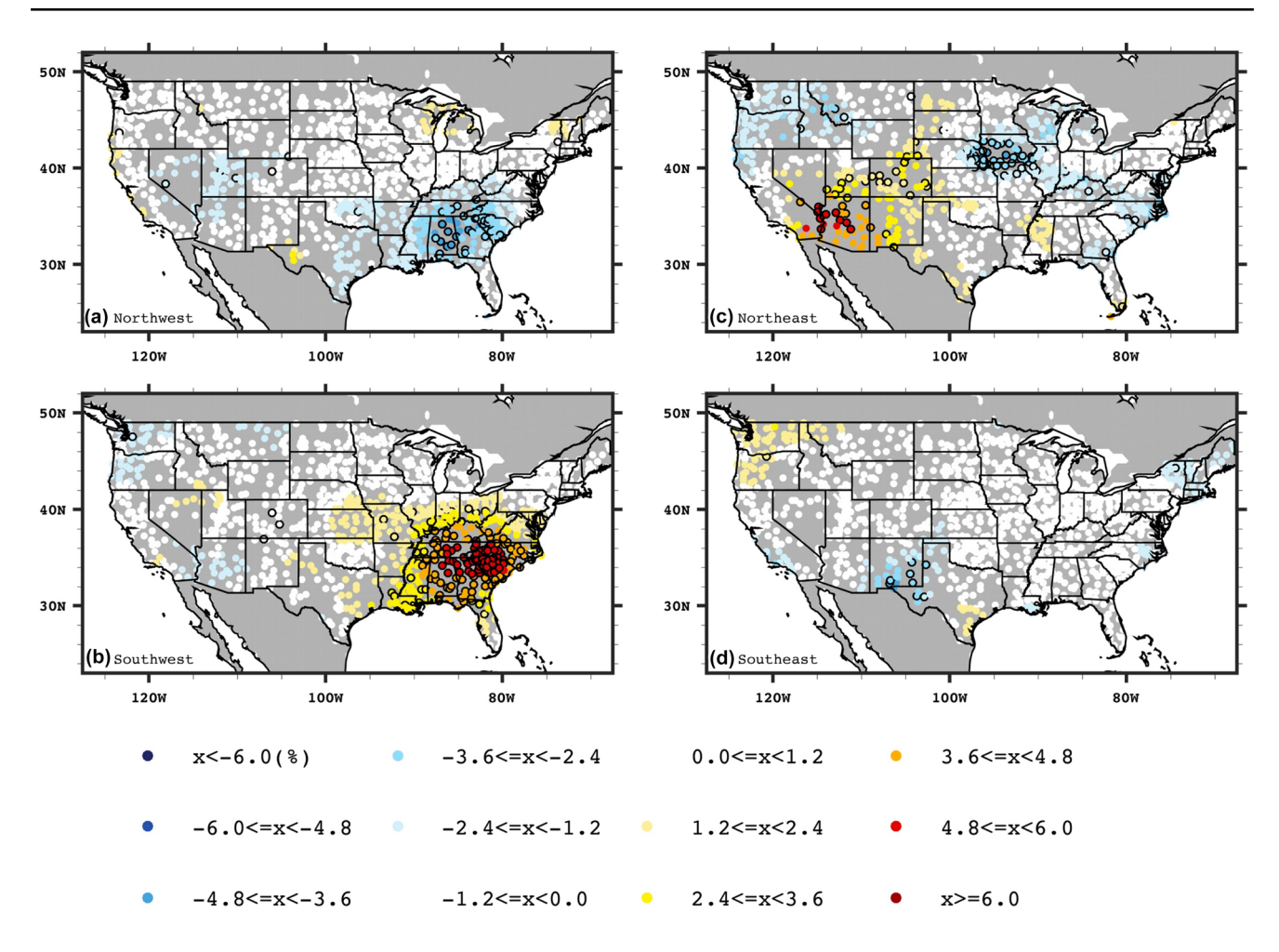
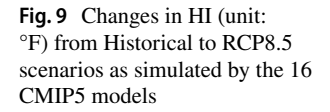
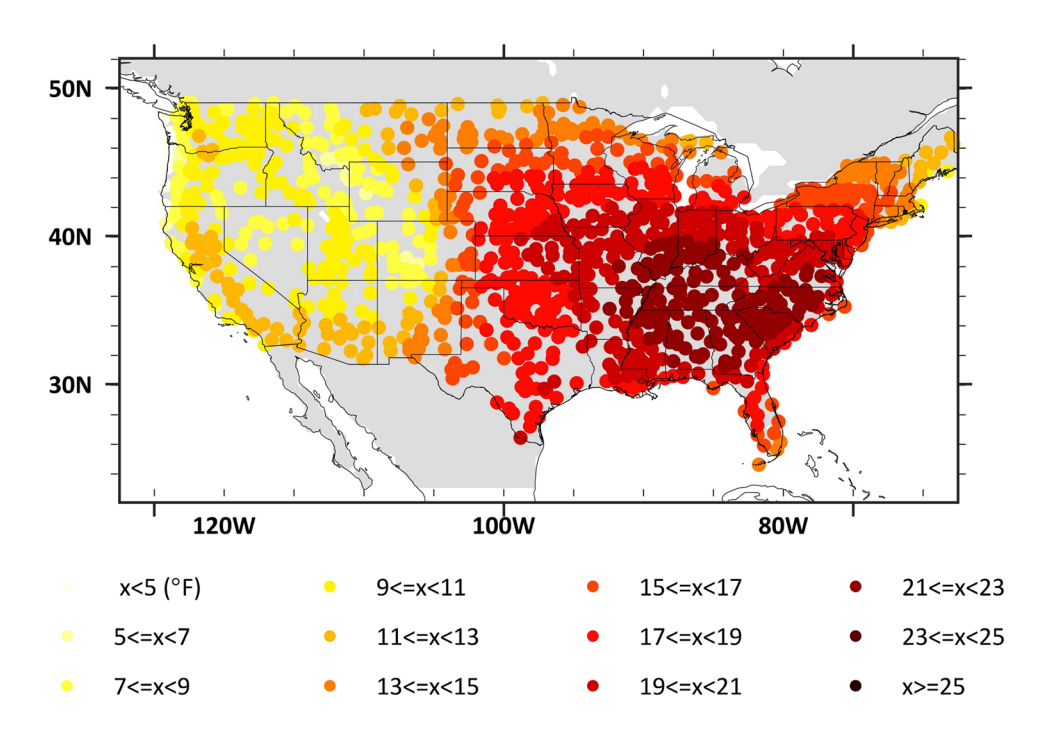


Fig. 8 Same as Fig. 4, but for cloud cover fraction derived from ISCCP-D2 during 1984–2009







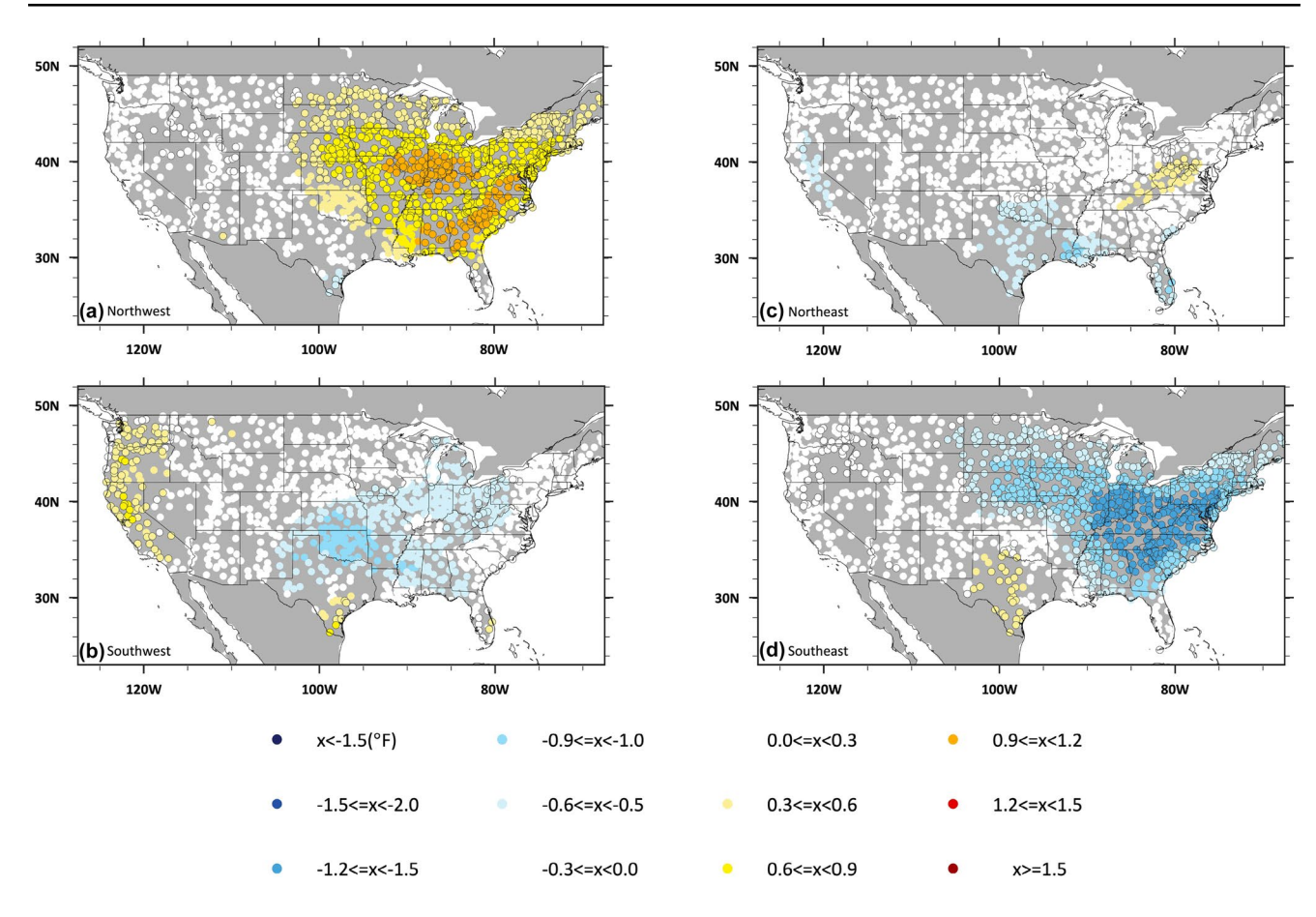
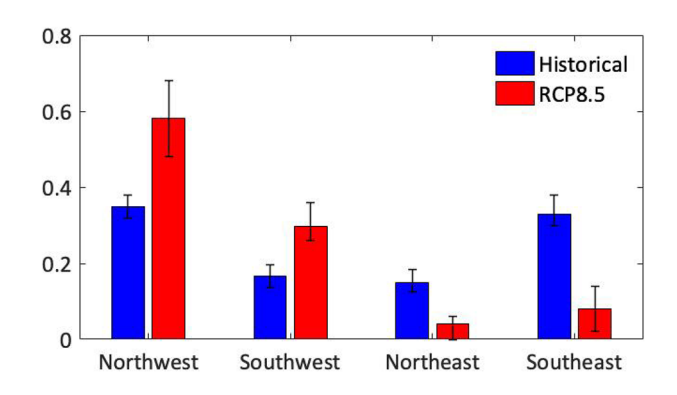


Fig. 10 Same as Fig. 4, but for HI (unit: °F) derived from Historical simulations of the 16 CMIP5 models during 1950–1999. Stations satisfying the criterion that at least 75% of the models have the same sign as the CMIP5 ensemble mean are plotted with black circles



**Fig. 11** Occurrence rate of NASH ridge types as simulated by the CMIP5 models under Historical and RCP8.5 scenarios. The bottom and top of each error bar shows the 25th and 75th percentile value among CMIP5 models

76% and 73%, similar to results present in Li et al. (2015) using RCP4.5 scenario.

The NASH-induced interannual variability of the HI tends to be weakened in the future except the SW summers (Fig. 12). Under the RCP8.5 scenario, the MME HI anomaly is about

0.5–1.2F higher over the area east of 105°W corresponding to the NW-type ridge, the higher HI (0.9–1.2F) area is mainly confined in the southern Appalachian region (Fig. 12a), smaller than that in the Historical simulation (Fig. 10a). Similarly, the projected HI anomaly is also weaker during the NE and SE ridge years (Fig. 12c, d). When the NASH ridge is located at the SW quadrant, the magnitude of negative HI anomaly enhances over the area east of 100°W, especially over the southeastern US where it drops by more than 30% (Fig. 12b).

In summary, in a warmer climate, the impact of NASH on the HI will be weakened over the area east of 100 W for the NW, SE, and NE ridge types; but the NASH may cause stronger negative HI anomalies when its ridge moves to the SW quadrant. The results suggest that the increased heat stress in the future could be caused by the background warming effect and NASH intensification.



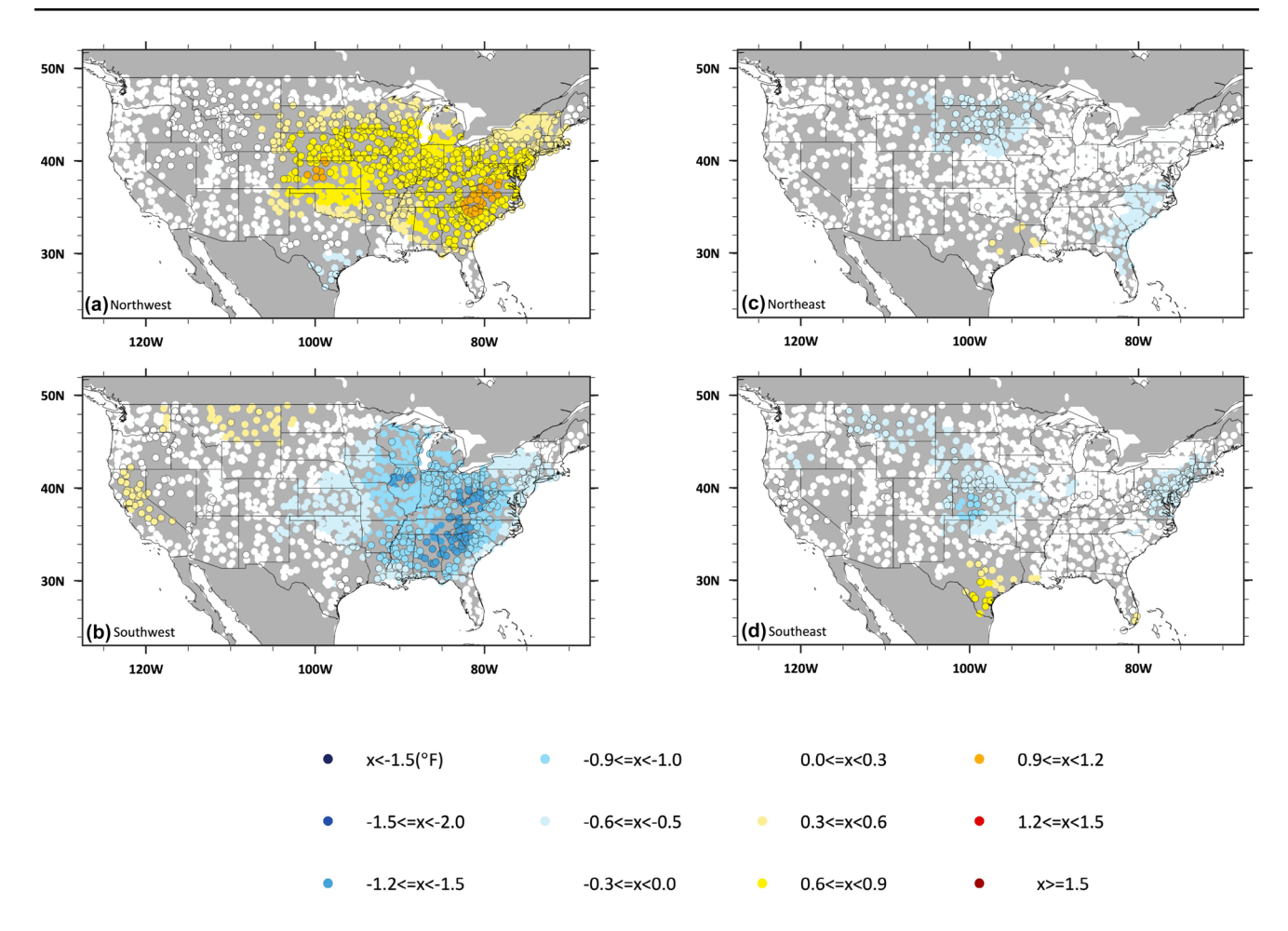


Fig. 12 Same as Fig. 10, but for detrended HI (unit: °F) derived from RCP8.5 simulations of the CMIP5 models during 2050–2099

### 4 Conclusion and discussion

The NASH plays an important role in altering *precipitation* over the conterminous *US in summer*. However, its impacts on HI over CONUS have not been systematically investigated. This study evaluates the impact of NASH on observed HI, the physical processes, and its implication for future HI.

Our analysis suggests that the HI is primarily controlled by air temperature in the CONUS; whereas RH is negatively correlated with the HI in western and Central US north of 40°N. In addition, atmospheric wind modulates HI over the Midwest and Southeastern US. These parameters, and thus the HI in the CONUS, are sensitive to the location change of the NASH western ridge. When the NASH western ridge is located northwest (NW) of its climatological mean position, abnormally high temperature is observed due to the reduction of clouds and deficit in precipitation. Although humidity does not significantly change during the NW ridge years, the increased temperature leads to positive HI anomalies over the Southeastern US. In contrast, when the western ridge is located in the southwest, anomalously low temperature is

observed over the Southeastern US which leads to negative HI although RH increases over the US east of 100 W. When the ridge is located at the NE quadrant, HI is characterized by weak negative anomalies over the Southeastern US and positive anomalies over the Northern United States east of 105°W; The HI does not significantly change when the NASH western ridge is located in the SE quadrant, indicating that the impact of NASH is weakened when it is far away from the North American continent with its ridge southward.

Under the future RCP 8.5 scenarios, CMIP5 models project HI to increase over the entire CONUS, especially east of 100°W. Meanwhile, the models project that the NASH-induced HI anomaly is weaker during the NW, NE, and SE ridge years, but stronger during SW years when the climate warms. The results suggest that the increased heat stress over the CONUS in the future is likely through both climatologically warming effect and the NASH intensification.

**Acknowledgements** We thank the international modeling groups for providing their data for analysis, the Program for Climate Model Diagnosis and Intercomparison (PCMDI) for collecting and archiving the model data, the JSC/CLIVAR Working Group on Coupled Modeling



(WGCM) and their Coupled Model Intercomparison Project (CMIP) and Climate Simulation Panel for organizing the model data analysis activity, and the IPCC WG1 TSU for technical support. The IPCC Data Archive at Lawrence Livermore National Laboratory is supported by the Office of Science, US Department of Energy. This work is supported by the NIH Grant NIH-1R21AG044294-01A1. L Li is supported by the NSF PREEVENTS (grant number: NSF-ICER-1663138).

### References

- Aguado E, Burt JE (2015) Understanding weather and climate, 7th edition. Pearson, London
- Arias PA, Fu R, Mo KC et al (2012) Decadal variation of rainfall seasonality in the North American Monsoon region and its potential causes. J Clim 25:4258–4274. https://doi.org/10.1175/JCLI-D-11-00140.1
- Berko J, Ingram DD, Saha S, Parker JD (2014) Deaths attributed to heat, cold, and other weather events in the United States, 2006–2010. Natl Health Stat Report 2014:1–15
- Biasutti M, Giannini A (2006) Robust Sahel drying in response to late 20th century forcings. Geophys Res Lett. https://doi. org/10.1029/2006GL026067
- Clement AC, Burgman R, Norris JR (2009) Observational and model evidence for positive low-level cloud feedback. Science 325:460–464. https://doi.org/10.1126/science.1171255
- Dave AC by, Susan Lozier M, Barber RT et al (2012) Physical controls on low and mid-latitude marine primary productivity
- Davis RE, Hayden BP, Gay DA et al (1997) The North Atlantic subtropical anticyclone. J Clim 10:728-744. https://doi.org/10.1175/1520-0442(1997)010%3C0728:TNASA %3E2.0.CO;2
- Easterling DR, Karl TR, Mason EH, Hughes PY, Bowman DP (1996)
  United States Historical Climatology Network (U.S. HCN)
  Monthly Temperature and Precipitation Data. Carbon Dioxide
  Information Analysis Center, Oak Ridge National Laboratory,
  U.S. Department of Energy, Oak Ridge, Tennessee
- Gamble DW, Curtis S (2008) Caribbean precipitation: review, model and prospect. Prog Phys Geogr 32:265–276. https://doi.org/10.1177/0309133308096027
- Ganguly AR, Steinhaeuser K, Erickson DJ et al (2009) Higher trends but larger uncertainty and geographic variability in 21st century temperature and heat waves. Proc Natl Acad Sci USA 106:15555– 15559. https://doi.org/10.1073/pnas.0904495106
- Gao Y, Fu JS, Drake JB et al (2012) Projected changes of extreme weather events in the eastern United States based on a high resolution climate modeling system. Environ Res Lett 7:044025. https://doi.org/10.1088/1748-9326/7/4/044025
- Gleckler PJ, Taylor KE, Doutriaux C (2008) Performance metrics for climate models. J Geophys Res Atmos. https://doi.org/10.1029/2007JD008972
- Grotjahn R, Black R, Leung R et al (2016) North American extreme temperature events and related large scale meteorological patterns: a review of statistical methods, dynamics, modeling, and trends. Clim Dyn 46:1151–1184. https://doi.org/10.1007/s0038 2-015-2638-6
- Intergovernmental Panel on Climate Change (2014) Climate change 2013—the physical science basis: Working Group I contribution to the fifth assessment report of the intergovernmental panel on climate change. Cambridge University Press, Cambridge
- Kalnay E, Kanamitsu M, Kistler R et al (1996) The NCEP/NCAR 40-year reanalysis project. Bull Am Meteorol Soc 77:437–471. https://doi.org/10.1175/1520-0477(1996)077%3C0437:TNYRP %3E2.0.CO;2

- Knowlton K, Rotkin-Ellman M, King G et al (2009) The 2006 California heat wave: impacts on hospitalizations and emergency department visits. Environ Health Perspect 117:61–67. https://doi.org/10.1289/ehp.11594
- Li W, Li L, Fu R et al (2011) Changes to the North Atlantic subtropical high and its role in the intensification of summer rainfall variability in the southeastern United States. J Clim 24:1499–1506. https://doi.org/10.1175/2010JCL13829.1
- Li L, Li W, Kushnir Y (2012a) Variation of the North Atlantic subtropical high western ridge and its implication to Southeastern US summer precipitation. Clim Dyn 39:1401–1412. https://doi.org/10.1007/s00382-011-1214-y
- Li W, Li L, Ting M, Liu Y (2012b) Intensification of Northern Hemisphere subtropical highs in a warming climate. Nat Geosci 5:830–834. https://doi.org/10.1038/ngeo1590
- Li L, Li W, Deng Y (2013a) Summer rainfall variability over the Southeastern United States and its intensification in the 21st century as assessed by CMIP5 models. J Geophys Res Atmos 118:340–354. https://doi.org/10.1002/jgrd.50136
- Li W, Li L, Ting M et al (2013b) Intensification of the Southern Hemisphere summertime subtropical anticyclones in a warming climate. Geophys Res Lett 40:5959–5964. https://doi.org/10.1002/2013GL058124
- Li L, Li W, Jin J (2015) Contribution of the North Atlantic subtropical high to regional climate model (RCM) skill in simulating south-eastern United States summer precipitation. Clim Dyn 45:477–491. https://doi.org/10.1007/s00382-014-2352-9
- Liu Y, Wu G (2004) Progress in the study on the formation of the summertime subtropical anticyclone. Adv Atmos Sci 21:322–342. https://doi.org/10.1007/BF02915562
- Meehl GA, Tebaldi C (2004) More intense, more frequent, and longer lasting heat waves in the 21st century. Science 305:994–997. https://doi.org/10.1126/science.1098704
- Minnesota Department of Health (2015) Heat-related illness weather. https://data.web.health.state.mn.us/hot\_weather. Accessed 27 Jun 2018
- National Weather Service (2017) 78-year list of severe weather fatalities. http://www.nws.noaa.gov/om/hazstats/resources/weather\_fatalities.pdf. Accessed 27 Jun 2018
- Nigam S, Chan SC (2009) On the summertime strengthening of the Northern Hemisphere Pacific sea level pressure anticyclone. J Clim 22:1174–1192. https://doi.org/10.1175/2008JCLI2322.1
- Peterson TC, Heim RR, Hirsch R et al (2013) Monitoring and understanding changes in heat waves, cold waves, floods, and droughts in the United States: state of knowledge. Bull Am Meteorol Soc 94:821–834. https://doi.org/10.1175/BAMS-D-12-00066.1
- Quinlan FT, Karl TR, Williams CN Jr (1987) United States Historical Climatology Network (HCN) Serial Temperature and Precipitation Data. NDP-019. Carbon Dioxide Information Analysis Center. Oak Ridge National Laboratory, U.S. Department of Energy, Oak Ridge, Tennessee
- Rossow WB, Schiffer RA (1991) ISCCP cloud data products. Bull Am Meteorol Soc 72:2–20. https://doi.org/10.1175/1520-0477(1991)072%3C0002:ICDP%3E2.0.CO;2
- Russo S, Sillmann J, Sterl A (2017) Humid heat waves at different warming levels. Sci Rep 7:7477. https://doi.org/10.1038/s4159 8-017-07536-7
- Smith TT, Zaitchik BF, Gohlke JM (2013) Heat waves in the United States: definitions, patterns and trends. Clim Change 118:811–825. https://doi.org/10.1007/s10584-012-0659-2
- Stahle DW, Cleaveland MK (1992) Reconstruction and analysis of spring rainfall over the Southeastern US for the past 1000 years. Bull Am Meteorol Soc 73:1947–1961. https://doi.org/10.1175/1520-0477(1992)073%3C1947:RAAOS R%3E2.0.CO;2



- Steadman RG (1979) The assessment of sultriness. Part I: a temperature-humidity index based on human physiology and clothing science. J Appl Meteorol 18:861–873. https://doi.org/10.1175/1520-0450(1979)018%3C0861:TAOSPI%3E2.0.CO;2
- Taylor KE, Stouffer RJ, Meehl GA et al (2012) An overview of CMIP5 and the experiment design. Bull Am Meteorol Soc 93:485–498. https://doi.org/10.1175/BAMS-D-11-00094.1
- Ting M, Wang H (1997) Summertime US precipitation variability and its relation to Pacific sea surface temperature. J Clim 10:1853–1873. https://doi.org/10.1175/1520-0442(1997)010%3C1853:SUSPVA%3E2.0.CO:2
- Trenberth KE, Shea DJ (2005) Relationships between precipitation and surface temperature. Geophys Res Lett. https://doi.org/10.1029/2005GL022760
- Vanos JK, Kalkstein LS, Sanford TJ (2015) Detecting synoptic warming trends across the US Midwest and implications to human health and heat-related mortality. Int J Climatol 35:85–96. https://doi.org/10.1002/joc.3964
- Wallace JM, Hobbs PV (2006) Atmospheric science: an introductory survey, 2nd ed. Academic Press, Burlington

- Wei W, Li W, Deng Y et al (2018a) Dynamical and thermodynamical coupling between the North Atlantic subtropical high and the marine boundary layer clouds in boreal summer. Clim Dyn 50:2457–2469. https://doi.org/10.1007/s00382-017-3750-6
- Wei W, Li W, Deng Y, Yang S (2018b) Intraseasonal variation of the summer rainfall over the Southeastern United States. Clim Dyn. https://doi.org/10.1007/s00382-017-3750-6
- Westcott NE (2011) The prolonged 1954 midwestern US heat wave: impacts and responses. Weather Clim Soc 3:165–176. https://doi.org/10.1175/WCAS-D-10-05002.1
- Whitman S, Good G, Donoghue ER et al (1997) Mortality in Chicago attributed to the July 1995 heat wave. Am J Public Health 87:1515–1518
- Wuebbles D, Meehl G, Hayhoe K et al (2013) CMIP5 climate model analyses: climate extremes in the United States. Bull Am Meteorol Soc 95:571–583. https://doi.org/10.1175/BAMS-D-12-00172.1

**Publisher's Note** Springer Nature remains neutral with regard to jurisdictional claims in published maps and institutional affiliations.

